

NUMERICAL SIMULATION OF FINITE DEFORMATIONS OF A DYNAMICALLY LOADED ELASTO-VISCOPLASTIC CIRCULAR MEMBRANE

W. D o r n o w s k i

Institute of Fundamental Technological Research,
Polish Academy of Sciences

21 Świętokrzyska Str., 00-049 Warsaw, Poland

The present paper deals with theoretical modeling and numerical simulation of a thin circular plate subjected to impulsive loading. To this end, the convective description is applied. The kinematical hypothesis used for theoretical description of the transient response includes membrane deformations only. This assumption is valid in the range of large deformations. The dynamical response of the material is described by Perzyna's elasto-viscoplastic constitutive relations. The theory is completed by an algorithm of the explicit finite difference method. With respect to the conditional stability of that method, the stability criterion is given. Basing on experimental data, an identification of material parameters is carried out. Some comparisons with the corresponding theoretical and experimental results are presented. Satisfactory agreement of the results has been found. Finally, an example of the plastic strain localization in a membrane is presented.

1. INTRODUCTION

The behavior of structures subjected to dynamic loads within the range of large inelastic strains is important for a broad class of engineering problems. In earlier works on the dynamical behavior of inelastic plates and membranes, some approximate methods were developed. These were initiated by the mode approximation solutions introduced by MARTIN and SYMONDS [19]. The approximation methods were developed for the case of small deflections, but when considering the effects of intense loading, the non-linearities due to large deflections must be taken into account. CHON and SYMONDS [4] proposed an extension of the original mode approximation solutions in order to account for finite deflections. SYMONDS and WIERZBICKI [26], GUEDES SOARES [12], PERRONE and BHADRA [22], LIPPMAN [17], BAKER [3] and NURICK *et al.* [21] used the mode approximation solutions in which the velocity field was assumed to be station-

ary. In this way they have solved a wide class of dynamic problems for inelastic, circular and rectangular plates and membranes.

The approximate methods presented in the mentioned papers account only for the basic effects of a deformation process such as the response duration and permanent transverse deflections. The simplicity and generality of these solutions are achieved by assumptions simplifying the analysis. Usually only the transverse motion of a membrane and the geometrical effects due to large rotations out of the middle surface are considered. As a result, the description of deformation corresponds to the geometrically linear theory.

However, the numerical approaches such as the finite element or finite difference methods allow for a more precise description of the deformation process. Solutions obtained in this way, though not so general as the analytical ones, can be based on more detailed theoretical formulations. Theory and problems of application of numerical methods in the nonlinear analysis of structures were presented by KLEIBER and WOŹNIAK [14], ARGYRIS *et al.* [1] and LEECH *et al.* [16]. The finite difference method for space and time presented by WITMER [28] should be admitted as very effective in numerical simulations of the inelastic, dynamical response of simple structural elements. The mixed analytical-numerical approach presented by BAK and DORNOWSKI in [2] and [5] can be very useful in problems of moderately large deflections of elastic-viscoplastic plates. The dynamical elasto-viscoplastic response of plates and shells was examined recently by KŁOSOWSKI *et al.* [15] and STOFFEL *et al.* [25]. In these papers, the material modeling accounts for elasto-plastic behavior, isotropic and kinematical hardening and strain-rate sensitivity. The numerical simulation of transient inelastic vibrations is performed using isoparametric finite elements.

In this paper, the analytical description of the finite deformations of a circular membrane is carried out in the convective coordinate system. The notion of the convective coordinate system is not new and it was used in several papers concerning the mechanics of continuum [9, 11, 13, 20]. In the convective description, the objective Lie derivative [18] of a spatial tensor field is represented by partial derivatives (with respect to time) of components of this tensor field [6, 8]. This property leads directly to the objective incremental formulations used in numerical algorithms.

In Sec. 2 a formulation of the problem is presented. In the framework of membrane theory used in considerations, no restrictions on the values of membrane strains are introduced. The equations of motion are derived in the deformed configuration. The relationships allowed to transform these equations to the initial configuration. The dynamical response of the membrane material is described by Perzyna's elasto-viscoplastic constitutive relations. The Huber-Mises yield condition and the associated viscoplastic flow rule are taken into account and the power overstress function is assumed.

The theory is completed by an algorithm of the explicit finite difference method, which is given in Sec. 3. An approach to the problem of discretization in space and time is presented. A numerical procedure of solution is developed in detail. With respect to the conditional stability of the proposed procedure, the stability criterion is given.

The subject of the numerical simulation presented in Sec. 4 is the circular membrane, which is made of the cold-rolled steel. Basing on the experimental data for this steel, an identification of material parameters is carried out. In the numerical way the solution convergence is proved. Some comparisons with the corresponding theoretical and experimental results are presented. Satisfactory agreement of the results is found. At the end of Sec. 4, an example of the plastic strain localization in the membrane is presented. Final comments and conclusions are given in Sec. 5.

2. FORMULATION OF THE PROBLEM

2.1. Geometrical relations

To analyze the finite deformation of a circular membrane, we assume the convective coordinate system $\{R, \Phi, Z\}$. At the initial time instant of motion, this coordinate system is cylindrical. Convective coordinates R and Φ are measured at the actual middle surface. The Z direction is assumed to be normal to the middle surface during the deformation.

The theoretical foundations on which the description of deformation in this note rests are as follows [6, 29]:

- The strain states of all material surfaces parallel to the middle surface are assumed to be identical (homogenous strain state).
- One of principal directions of the strain at every point of the membrane remains orthogonal to the middle surface during the deformation.

These assumptions imply that only membrane deformations can develop, while the bending and shear effects are neglected. It should be stressed that the above foundations do not impose any limitations on the magnitude of strains induced in the membrane. On the contrary, they have much wider use in the framework of the finite deformation theory. In the thin plate subjected to large deformations, the membrane states dominate while the bending states have a meaning only at the beginning of the deformation process.

Thus the deformation of the membrane can be defined by the first and second metric tensors of the middle surface. In the technically important problem of the axisymmetric deformation, these tensors can be written in the following matrix form:

$$(2.1) \quad \mathbf{g} = \begin{bmatrix} r_{,R}^2 + z_{,R}^2 & 0 \\ 0 & r^2 \end{bmatrix},$$

$$\mathbf{b} = \begin{bmatrix} (r_{,R} z_{,RR} - r_{,RR} z_{,R}) / (r_{,R}^2 + z_{,R}^2)^{1/2} & 0 \\ 0 & r z_{,R} / (r_{,R}^2 + z_{,R}^2)^{1/2} \end{bmatrix},$$

where r and z denote the components of the position vector of the midsurface in the initial configuration. Comma denotes partial differentiation with respect to the spatial, convective coordinates. The metric tensors for the undeformed, initially flat membrane are given by

$$(2.2) \quad \mathbf{G} = \begin{bmatrix} 1 & 0 \\ 0 & R^2 \end{bmatrix}, \quad \mathbf{B} = \begin{bmatrix} 0 & 0 \\ 0 & 0 \end{bmatrix}.$$

The strain state in the thin membrane can be described by the Almansi tensor as follows:

$$(2.3) \quad \mathbf{e} = \frac{1}{2}(\mathbf{g} - \mathbf{G}) = \begin{bmatrix} (r_{,R}^2 + z_{,R}^2 - 1)/2 & 0 \\ 0 & (r^2 - R^2)/2 \end{bmatrix}.$$

The radial and circumferential strains are respectively determined by the non-zero components of the tensor (2.3).

2.2. Equations of motion

The tensor of membrane forces is

$$(2.4) \quad \mathbf{n} = h \begin{bmatrix} \sigma^{RR} & 0 \\ 0 & \sigma^{\Phi\Phi} \end{bmatrix},$$

where h denotes the thickness of the deformed membrane, σ^{RR} and $\sigma^{\Phi\Phi}$ denote the radial and circumferential components of the Cauchy stress tensor, respectively. Motion of the circular membrane exposed to the transverse pressure $p(R, t)$ is described by the following equations:

$$(2.5) \quad \begin{aligned} \mu a^R &= n^{RR}_{,R} + (2\gamma_{RR}^R + \gamma_{R\Phi}^\Phi) n^{RR} + \gamma_{\Phi\Phi}^R n^{\Phi\Phi}, \\ \mu \lambda a^z &= b_{RR} n^{RR} + b_{\Phi\Phi} n^{\Phi\Phi} + p. \end{aligned}$$

Here, except the quantities prescribed before, we have components of the acceleration vector denoted by a^R and a^z , $\lambda = h/H$ denotes the actual, initial

thickness ratio, $\mu = \rho h$ is the mass density per unit area of the deformed middle surface. Christoffel's symbols are given by the relations

$$(2.6) \quad \gamma_{RR}^R = \frac{r_{,R} r_{,RR} + z_{,R} z_{,RR}}{r_{,R}^2 + z_{,R}^2}, \quad \gamma_{\Phi\Phi}^R = -\frac{r r_{,R}}{r_{,R}^2 + z_{,R}^2}, \quad \gamma_{R\Phi}^\Phi = \frac{r_{,R}}{r}.$$

The equations of motion (2.5) are prescribed in the actual configuration metrics. They can be transformed to the initial configuration as follows

$$(2.7) \quad \begin{aligned} \ddot{r} &= r_{,R} a^R - \lambda a^Z z_{,R} / (r_{,R}^2 + z_{,R}^2)^{1/2}, \\ \ddot{z} &= z_{,R} a^R + \lambda a^Z r_{,R} / (r_{,R}^2 + z_{,R}^2)^{1/2}. \end{aligned}$$

Thus \ddot{r} and \ddot{z} denote the radial and normal components of the acceleration vector with respect to the initial membrane configuration. Dot denotes partial differentiation with respect to the time coordinate.

2.3. Constitutive relations

The constitutive relations create the remaining relations describing the considered problem. The rate-type, elasto-viscoplastic constitutive relations formulated by Perzyna in [23] are used. The considerations are limited to the isotropic materials without plastic hardening. Because the problems of failure are not considered, the nucleation and microcrack growth are neglected.

The formulation of the material law starts with the assumption that the strain rates can be additively decomposed into elastic and plastic parts,

$$(2.8) \quad \dot{e}_{RR} = \dot{e}_{RR}^e + \dot{e}_{RR}^p, \quad \dot{e}_{\Phi\Phi} = \dot{e}_{\Phi\Phi}^e + \dot{e}_{\Phi\Phi}^p$$

For the isotropic, linear elastic behavior and for the plane stress conditions, the elastic strain rates can be derived from the relations

$$(2.9) \quad \begin{aligned} \dot{\sigma}^{RR} &= \frac{E}{1-\nu^2} [\dot{e}_{RR}^e (g^{RR})^2 + \nu \dot{e}_{\Phi\Phi}^e g^{RR} g^{\Phi\Phi}], \\ \dot{\sigma}^{\Phi\Phi} &= \frac{E}{1-\nu^2} [\dot{e}_{\Phi\Phi}^e (g^{\Phi\Phi})^2 + \nu \dot{e}_{RR}^e g^{RR} g^{\Phi\Phi}]. \end{aligned}$$

where g^{RR} and $g^{\Phi\Phi}$ denote the contravariant components of the first metric tensor of the deformed middle surface, E denotes Young's modulus and ν is Poisson's ratio.

The viscoplastic flow process starts when the stress state attains the initial yield surface described by the equation

$$(2.10) \quad \varphi = f/\sigma_0 - 1 = 0$$

where σ_0 denotes the uniaxial yield stress, and the Huber-Mises plastic potential function is

$$(2.11) \quad f = [(\sigma^{RR}g_{RR})^2 + (\sigma^{\Phi\Phi}g_{\Phi\Phi})^2 - \sigma^{RR}\sigma^{\Phi\Phi}g_{RR}g_{\Phi\Phi}]^{1/2}.$$

The normality rule for plastic flow, which describes inelastic material properties, is defined by

$$(2.12) \quad \begin{aligned} \dot{e}_{RR}^p &= \Lambda [2\sigma^{RR}(g_{RR})^2 - \sigma^{\Phi\Phi}g_{RR}g_{\Phi\Phi}], \\ \dot{e}_{\Phi\Phi}^p &= \Lambda [2\sigma^{\Phi\Phi}(g_{\Phi\Phi})^2 - \sigma^{RR}g_{RR}g_{\Phi\Phi}]. \end{aligned}$$

The scalar multiplier Λ is determined by the expression

$$(2.13) \quad \Lambda = \frac{\gamma}{\sqrt{3}\xi f} \langle \varphi^\delta \rangle.$$

where constant γ denotes the viscosity parameter and φ^δ is the assumed over-stress function, such that

$$(2.14) \quad \langle \varphi^\delta \rangle = \begin{cases} 0 & \text{for } \varphi \leq 0 \\ \varphi^\delta & \text{for } \varphi > 0. \end{cases}$$

The function ξ , which controls the plastic flow process [23], is assumed in the form

$$(2.15) \quad \xi = \left(\sqrt{I_2}/\sqrt{I_2^s} - 1 \right)^\beta$$

where

$$(2.16) \quad I_2 = [(\dot{e}_{RR}g^{RR})^2 + (\dot{e}_{\Phi\Phi}g^{\Phi\Phi})^2 + \dot{e}_{RR}^p\dot{e}_{\Phi\Phi}^p g^{RR}g^{\Phi\Phi} + I_2^p] / 2$$

is the second invariant of the entire deformation rate. In Eq. (2.16) the assumption of plastic incompressibility is included, however, the insignificant influence of the component $\dot{e}_{zz}^e = \lambda^2[\dot{e}_{RR}^p g^{RR} + \dot{e}_{\Phi\Phi}^p g^{\Phi\Phi} - \nu(\dot{\sigma}^{RR}g_{RR} + \dot{\sigma}^{\Phi\Phi}g_{\Phi\Phi})/E]$ has been neglected. For example, it is shown in Fig. 5 how the component \dot{e}_{zz}^e influences the evolution of the midpoint deflection. The second invariant of the plastic deformation rate can be written as

$$(2.17) \quad I_2^p = \dot{e}_{RR}^p (\dot{e}_{RR}^p g^{RR}g^{RR} + \dot{e}_{\Phi\Phi}^p g^{RR}g^{\Phi\Phi}) + (\dot{e}_{\Phi\Phi}^p g^{\Phi\Phi})^2.$$

By I_2^s we have denoted such a value of the invariant (2.16) for which the rate effects are small (statical case). The control function (2.15) has the following features:

$$(2.18) \quad \xi(0) = 0 \quad \text{and} \quad \xi(\cdot) = 0 \quad \text{for} \quad I_2 < I_2^s.$$

The change of the plastic yield surface in the stress space is determined by the dynamical yield condition

$$(2.19) \quad \Theta = f - \sigma_0 \left[1 + \left(\frac{\xi \sqrt{I_2^p}}{\gamma} \right)^{1/\delta} \right] = 0.$$

It is noteworthy that the constitutive relations considered above take into account changes of the membrane geometry due to the whole deformation. If we assume in all the constitutive relations that

$$(2.20) \quad g_{RR} = G_{RR}, \quad g_{\phi\phi} = G_{\phi\phi}, \quad g^{RR} = G^{RR}, \quad g^{\phi\phi} = G^{\phi\phi},$$

we will obtain the constitutive relations that are mainly used in the problems of infinitesimal elasto-viscoplastic strains. Such an assumption is equivalent to neglecting the geometrical non-linearities.

Making use of the property of plastic incompressibility, we can calculate the membrane actual thickness as follows:

$$(2.21) \quad h = HR [(2e_{RR}^p + 1)(2e_{\phi\phi}^p + R^2)]^{-1/2}.$$

2.4. Initial-boundary conditions

To formulate completely the problem of inelastic membrane dynamics posed in this way, we have to prescribe suitable boundary and initial conditions. For the considered membrane, the boundary conditions express the fact that all displacements vanish at the membrane boundary. The form of initial conditions depends on the type of the assumed external loading. For the initial velocity impulse V_0 , which is assumed in our numerical example, the equations of motion are homogeneous ($p = 0$), and the initial conditions are given by

$$(2.22) \quad r(R, 0) = R, \quad z(R, 0) = 0, \quad \dot{r}(R, 0) = 0, \quad \dot{z}(R, 0) = V_0.$$

These conditions concern the membrane assumed to be initially flat.

3. METHOD OF SOLUTION

3.1. Discretization in space and time

For solving that initial-boundary value problem, the explicit difference method is used including both the time and membrane discretizations. The whole system of equations containing the geometrical relations, equations of motion, constitutive relations and the evolution equation for the membrane thickness has been analyzed numerically.

Using the axial symmetry of the problem, we begin by subdividing the membrane region into N ring segments of identical widths ΔR (Fig. 1).

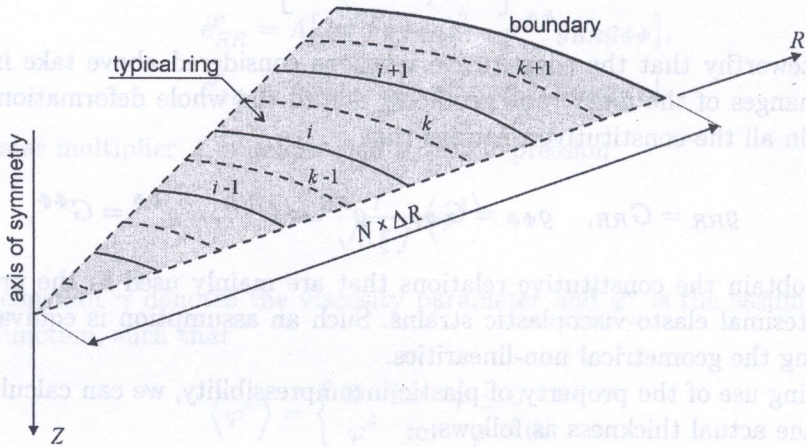


FIG. 1. Subdivision of the membrane region into N ring segments.

As a result of this subdivision, we obtain the collection of nodal circles (i). Furthermore, we introduce the collection of indirect circles (k) at the same distance from the nodal circles. It is very important to notice that in the preferred convective description, the discretization parameter ΔR has a constant value during the whole motion, while the material line element, which has the initial length $\Delta S = \Delta R$, is subjected to deformation. The first metric tensor $(2.1)_1$ of the deformed membrane is a measure of this deformation. Next, we replace time by the discrete set of time instants $t^n, n = 1, 2, 3, \dots$, assuming the constant time step $\Delta t = t^n - t^{n-1}$.

3.2. Numerical procedure of solution

In order to start the cyclic procedure it is assumed that at the actual time instant t^n , the membrane configuration is given by the position vector of nodal

circles (i). To determine the strain state (2.3), the knowledge of gradients $r_{,R}$ and $r_{,Z}$ is required. These gradients are calculated for the indirect nodal circles (k) by using the following finite difference formulas:

$$(3.1) \quad \left. r_{,R} \right|_k^n = (r_{i+1}^n - r_i^n) / \Delta R,$$

$$\left. z_{,R} \right|_k^n = (z_{i+1}^n - z_i^n) / \Delta R.$$

The strain increments between time instants t^{n-1} and t^n are also calculated for the indirect nodal circles (k), according to these differences

$$(3.2) \quad \left. \Delta e_{RR} \right|_k^{n,n-1} = e_{RR} \Big|_k^n - e_{RR} \Big|_k^{n-1},$$

$$\left. \Delta e_{\Phi\Phi} \right|_k^{n,n-1} = e_{\Phi\Phi} \Big|_k^n - e_{\Phi\Phi} \Big|_k^{n-1}.$$

From the strain increments, the stress increments, are determined by using suitable constitutive relations, and they are added to the already existing stresses as follows:

$$(3.3) \quad \left. \sigma_{RR} \right|_k^n = \left. \sigma_{RR} \right|_k^{n-1} + \left. \Delta \sigma_{RR} \right|_k^{n,n-1},$$

$$\left. \sigma_{\Phi\Phi} \right|_k^n = \left. \sigma_{\Phi\Phi} \right|_k^{n-1} + \left. \Delta \sigma_{\Phi\Phi} \right|_k^{n,n-1}.$$

The stress increments $\left. \Delta \sigma_{RR} \right|_k^{n,n-1}$ and $\left. \Delta \sigma_{\Phi\Phi} \right|_k^{n,n-1}$ are calculated from the incremental form of (2.9) where increments of total strains (3.2) are treated as elastic. The correctness of such a procedure is assured if $\varphi|_k^n \leq 0$. If this inequality is satisfied, it means that the elastic strain process is realized at the considered ring segment. It may be the loading or unloading process proceeding in the purely or secondarily elastic region. In the case when $\varphi|_k^n > 0$, the stresses calculated according to Eq. (3.3) should be treated as so-called trial stresses denoted by $\bar{\sigma}_{RR}$ and $\bar{\sigma}_{\Phi\Phi}$.

By applying the additive structure of that incremental constitutive relations we obtain the relationships between stresses suitable for the elasto-plastic state and the trial stresses,

$$(3.4) \quad \sigma^{RR} \Big|_k^n = \frac{1}{1 + \nu + 3E\Lambda} \left[(1 + \nu) \bar{\sigma}^{RR} + \frac{(1 - 2\nu)E\Lambda}{1 - \nu + E\Lambda} (\bar{\sigma}^{RR} + \bar{\sigma}^{\Phi\Phi} g^{RR} g_{\Phi\Phi}) \right] \Big|_k^n$$

$$(3.4) \quad \sigma^{\Phi\Phi} \Big|_k^n = \frac{1}{1 + \nu + 3E\Lambda} \left[(1 + \nu) \bar{\sigma}^{RR} + \frac{(1 - 2\nu)E\Lambda}{1 - \nu + E\Lambda} (\bar{\sigma}^{\Phi\Phi} + \bar{\sigma}^{RR} g^{\Phi\Phi} g_{RR}) \right] \Big|_k^n$$

This system of algebraic equations will be appointed with respect to the scalar multiplier if we will add to it the dynamical yield condition

$$(3.5) \quad \Theta(\Lambda) \Big|_k^n = 0.$$

With respect to the non-linearity of this condition, the scalar multiplier Λ has to be determined by one of the iterative methods, e.g. Newton's method for which the following iterative procedure holds:

$$(3.6) \quad \Lambda_{(r+1)} = \Lambda_{(r)} - \left[\frac{\partial \Theta(\Lambda_{(r)}) \Big|_k^n}{\partial \Lambda_{(r)}} \right]^{-1} \Theta_k^n(\Lambda_{(r)}) \Big|_k^n, \quad r = 0, 1, 2, \dots$$

This procedure starts at the initial value $\Lambda_{(0)} = 0$ and it stops when the following condition is satisfied

$$(3.7) \quad |\Lambda_{(r+1)} - \Lambda_{(r)}| < \varepsilon,$$

where ε denotes a preset convergence tolerance of Λ . Once the iterative procedure is finished, we obtain the stresses as well as the plastic and elastic strain increments at the indirect node circles (k).

Plastic strains

$$(3.8) \quad e_{RR}^p \Big|_k^n = e_{RR}^p \Big|_k^{n-1} + \Delta e_{RR}^p \Big|_k^{n,n-1}, \quad e_{\Phi\Phi}^p \Big|_k^n = e_{\Phi\Phi}^p \Big|_k^{n-1} + \Delta e_{\Phi\Phi}^p \Big|_k^{n,n-1},$$

cause a change of the membrane thickness

$$(3.9) \quad h \Big|_k^n = HR \left[(2e_{RR}^p \Big|_k^n + 1)(2e_{\Phi\Phi}^p \Big|_k^n + R_k^2) \right]^{-1/2}.$$

Knowing the stress state as well as the actual membrane thickness, we can calculate the membrane forces according to (2.4).

Components of the acceleration field connected with the actual configuration are calculated for the set of nodal circles (i) according to the equations of motion (2.5). Spatial derivatives included in these equations are replaced by the following difference quotients:

$$(3.10) \quad \begin{aligned} n^{RR},R \Big|_i^n &= (n^{RR} \Big|_k^n - n^{RR} \Big|_{k-1}^n) / \Delta R, & r_{,R} \Big|_i^n &= (r_{i+1}^n - r_{i-1}^n) / \Delta R / 2, \\ z_{,R} \Big|_i^n &= (z_{i+1}^n - z_{i-1}^n) / \Delta R / 2, & r_{,RR} \Big|_i^n &= (r_{i-1}^n - 2r_i^n + r_{i+1}^n) / \Delta R^2, \\ z_{,RR} \Big|_i^n &= (z_{i-1}^n - 2z_i^n + z_{i+1}^n) / \Delta R^2, \end{aligned}$$

Using the transforming formulas (2.7) we can calculate the acceleration field components \ddot{r}_i^n and \ddot{z}_i^n in the initial configuration. To determine the membrane configuration at the next time instant of motion, the centered difference quotients is used as follows

$$(3.11) \quad r_i^{n+1} = \Delta t^2 \ddot{r}_i^n + 2r_i^n - r_i^{n+1}, \quad z_i^{n+1} = \Delta t^2 \ddot{z}_i^n + 2z_i^n - z_i^{n+1}$$

An advantage of the proposed method of solution is the recursive character of calculations; therefore, there is no problem of time-consuming solution of the set of nonlinear algebraic equations at every time step. This problem has to be solved in the case of implicit formulations. Instead, here the conditional stability is the basic difficulty. The time step assuring stability should be smaller than certain critical time step Δt_{cr} , which depends on properties of the whole discretized system. The harmonic analysis of Eqs. (3.11) leads to a conclusion that to assure the absolute stability, it has to be

$$(3.12) \quad \Delta t \leq \Delta t_{cr} = 2/\omega,$$

where ω denotes the highest frequency of the natural vibration of a discretized structure. In the considered, generally nonlinear problem, this frequency depends on deformation. Thus, the critical value (3.12) is changing during the deformation process, but it is possible to estimate the constant value of Δt_{cr} by analyzing the suitable linear problem.

To start the calculations, a special starting procedure must be used. For the homogeneous transverse initial velocity V_0 we obtain

$$(3.13) \quad z_i^1 = V_0 \Delta t.$$

This may be interpreted as the difference form of initial conditions for this case of loading.

4. NUMERICAL EXAMPLE

4.1. Identification of material parameters

The subject of this numerical simulation is the circular membrane of dimensions:

$$A = 50 \text{ mm} \text{ -- radius,}$$

$$H = 1.6 \text{ mm} \text{ -- thickness.}$$

The membrane is made from the cold-rolled mild steel. Some thin steel plates of such dimensions were investigated theoretically and experimentally in [27]. The Metabel sheet explosive used was arranged using a two ring configuration interconnected by a cross leader, and was placed on a polystyrene pad in order to provide a uniform impulse and prevent spallation of the specimen. It is reported that as the impulse was increased, three distinctly different damage modes were noted:

mode I : large inelastic deformation,

mode II : tearing (tensile failure) in outer fibres, at or over the support,

mode III: transverse shear failure at the support.

Some comparisons presented below with the corresponding theoretical and experimental results relate to the first damage mode (large inelastic deformation). The plates tested in [27] were cut from two cold-rolled mild steel sheets and were clamped to the pendulum in such a way as to allow the impulsive load to be distributed over a circular area having a radius of 50 mm. From these sheets, the two groups of specimens were also prepared, and next they were subjected to tensile tests. Three different strain rates were used. The values of the upper yield stress σ_u associated with applied strain rates are listed in Table 1.

Table 1. Experimental data of mild steel tensile tests.

sheet I, $\sigma_0 = 264\text{MPa}$		sheet II, $\sigma_0 = 277\text{MPa}$	
$\dot{\epsilon}[\text{s}^{-1}]$	$\sigma_u[\text{MPa}]$	$\dot{\epsilon}[\text{s}^{-1}]$	$\sigma_u[\text{MPa}]$
$3.33 \cdot 10^{-4}$	266	$3.33 \cdot 10^{-4}$	284
$1.33 \cdot 10^{-3}$	288	$1.33 \cdot 10^{-3}$	320
$6.67 \cdot 10^{-3}$	300	$6.67 \cdot 10^{-3}$	350

The data listed in Table 1, at least strongly limited, are used in the identification procedure of the assumed constitutive model. The dynamic yield condition

(2.19) is assumed to be a basis for this identification. For the uniaxial case it has the form

$$(4.1) \quad \sigma_d = \eta^{-2} \sigma_0 \left\{ 1 + \left[\eta^{-2} \frac{\dot{\epsilon}^p}{\gamma_0} \left(\frac{\dot{\epsilon}}{\dot{\epsilon}_s} - 1 \right)^\beta \right]^{1/\delta} \right\},$$

where η denotes the specimen extension, i.e. the initial-actual gauge length ratio. The upper yield stress is already attained at the extension $\eta \cong 1.002$; thus the influence of can be neglected in Eq. (4.1). In such a case the Cauchy stress can be identified with the nominal stress, while the deformation rate corresponds to the engineering strain rate. Both these measures are used for representing the results of the tensile tests.

To identify the material parameters γ_0 , β and δ the best curve fitting of the upper yield stress-strain rate relation is carried out (see Fig. 2). The obtained results are listed in Table 2.

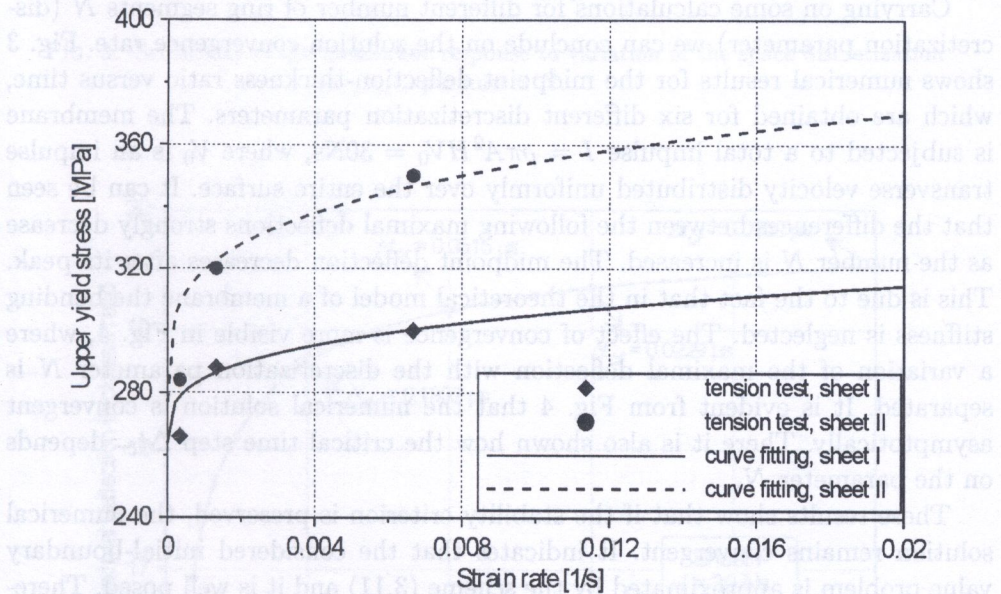


FIG. 2. Variation of the upper yield stress with strain rate for the mild steel specimen.

4.2. Stability and convergence

As it has been described, the time step assuring the stability should be smaller than certain critical time step Δt_{cr} , which depends on deformation. To estimate

Table 2. Material parameters for the mild steel.

parameters	sheet I	sheet II
σ_0	264 MPa	277 MPa
$\dot{\epsilon}_s$	10^{-6} s^{-1}	10^{-6} s^{-1}
γ_0	12000 s^{-1}	2.6 s^{-1}
δ	5.0	4.0
β	0.51	0.05

the constant, protected value of Δt_{cr} the suitable linear problem is analyzed and the following value is obtained

$$(4.2) \quad \Delta t_{cr} = \Delta R \sqrt{\frac{\rho(1 - \nu^2)}{E}}.$$

In all the numerical calculations, for an additional safety, it is assumed that $\Delta t = 0.7\Delta t_{cr}$.

Carrying on some calculations for different number of ring segments N (discretization parameter) we can conclude on the solution convergence rate. Fig. 3 shows numerical results for the midpoint deflection-thickness ratio versus time, which are obtained for six different discretization parameters. The membrane is subjected to a total impulse $I = \rho\pi A^2 HV_0 = 30\text{Ns}$, where V_0 is an impulse transverse velocity distributed uniformly over the entire surface. It can be seen that the differences between the following maximal deflections strongly decrease as the number N is increased. The midpoint deflection decreases after its peak. This is due to the fact that in the theoretical model of a membrane the bending stiffness is neglected. The effect of convergence is more visible in Fig. 4, where a variation of the maximal deflection with the discretization parameter N is separated. It is evident from Fig. 4 that the numerical solution is convergent asymptotically. There it is also shown how the critical time step Δt_{cr} depends on the parameter N .

These results show that if the stability criterion is preserved, the numerical solution remains convergent. It indicates that the considered initial-boundary value problem is approximated by the scheme (3.11) and it is well posed. Therefore, these results may be treated as a numerical proof of the Lax-Richtmyer equivalence theorem [24]. If the stability criterion is not preserved the unrestricted growth of amplitudes of considered functions takes place already for first several time increments.

In Fig. 5 the influence of the normal component $\dot{\epsilon}_{zz}^e$ of elastic strain rate on the midpoint deflection is shown. One can be noticed that this influence on the maximal midpoint deflection is very slight and can be neglected in the considered case. Some differences are visible in the elastic unloading range.

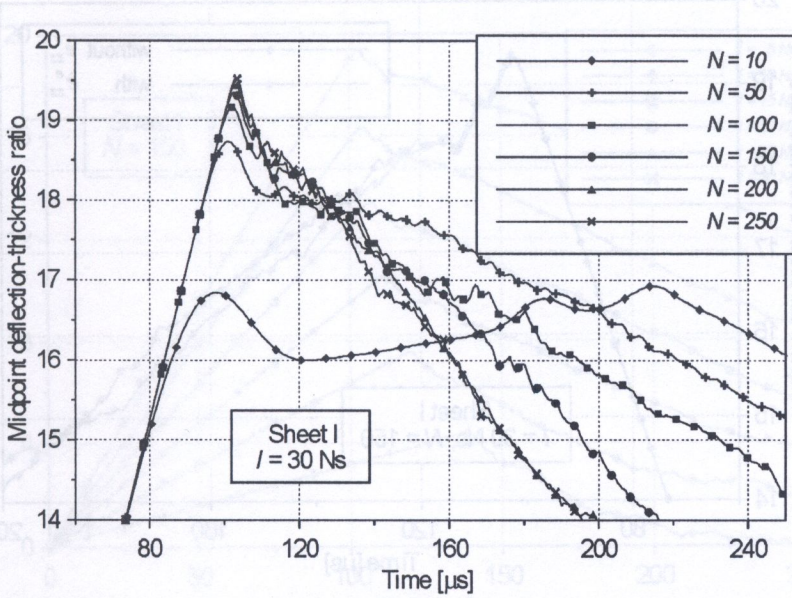


FIG. 3. Sensitivity of the membrane response to variation of the space discretization parameter N .

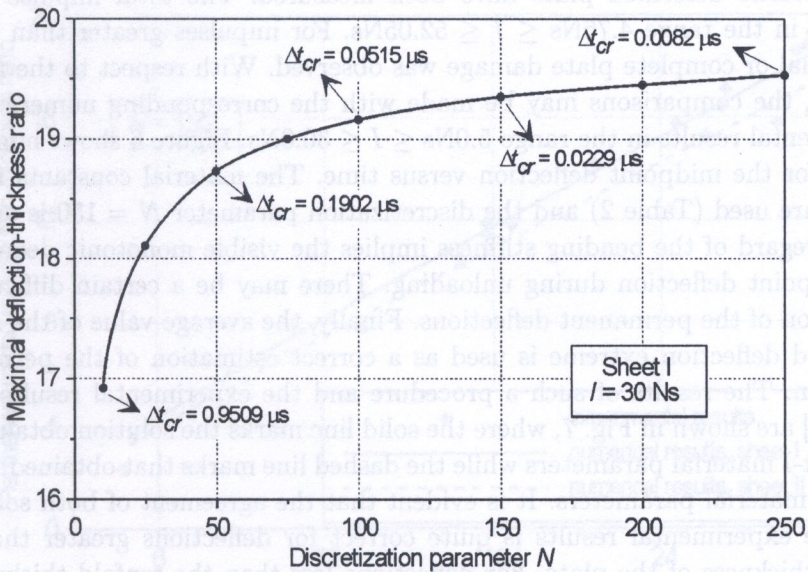


FIG. 4. Variation of the maximal deflection with the discretization parameter N as an illustration of the solution convergence.

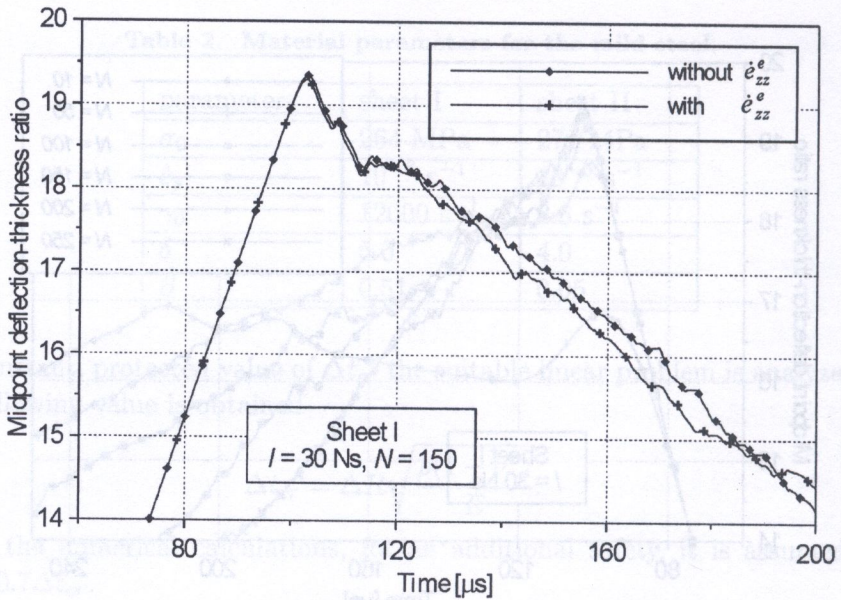


FIG. 5. Influence of the component $\dot{\epsilon}_{zz}^e$ on the midpoint deflection.

4.3. Numerical results versus experimental data

In the experiments reported in [27] the final midpoint deflection and a shape of the plastic deformed plate have been measured. The total impulse I was changed in the range $4.76\text{Ns} \leq I \leq 52.05\text{Ns}$. For impulses greater than 30 Ns, the partial or complete plate damage was observed. With respect to the mode-I analysis, the comparisons may be made with the corresponding numerical and experimental results in the range $5.0\text{Ns} \leq I \leq 30.0\text{Ns}$. Figure 6 shows numerical results for the midpoint deflection versus time. The material constants for the sheet I are used (Table 2) and the discretization parameter $N = 150$ is applied. The disregard of the bending stiffness implies the visible monotonic decrease of the midpoint deflection during unloading. There may be a certain difficulty in estimation of the permanent deflections. Finally, the average value of the second and third deflection extreme is used as a correct estimation of the permanent deflection. The results of such a procedure and the experimental results taken from [27] are shown in Fig. 7, where the solid line marks the solution obtained for the sheet-I material parameters while the dashed line marks that obtained for the sheet-II material parameters. It is evident that the agreement of both solutions with the experimental results is quite correct for deflections greater than the tenfold thickness of the plate. For deflections less than the tenfold thickness of the plate, all experimental points lie below these theoretical lines. It means that in the deflection range to the tenfold thickness the bending effects, which have been omitted in the theoretical formulation, play an important role.

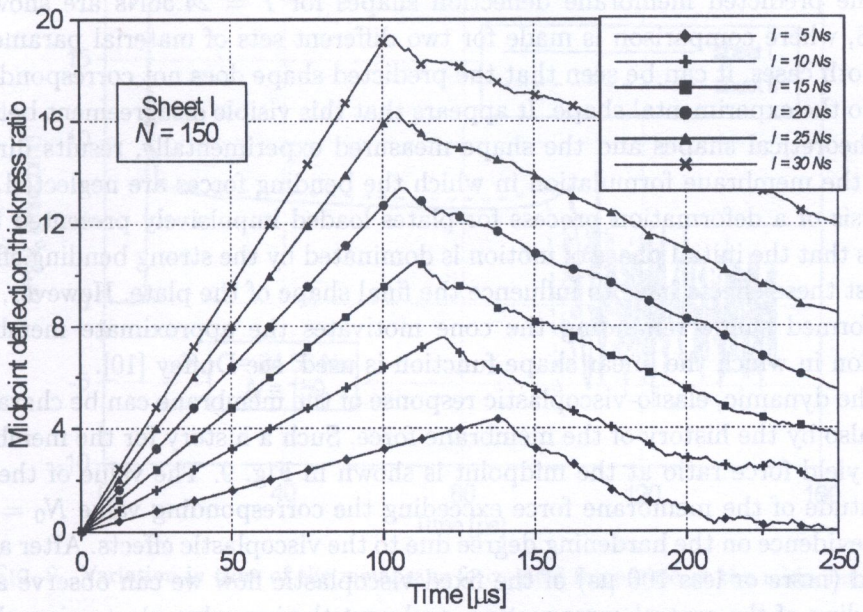


FIG. 6. Midpoint deflection-thickness ratio versus time.

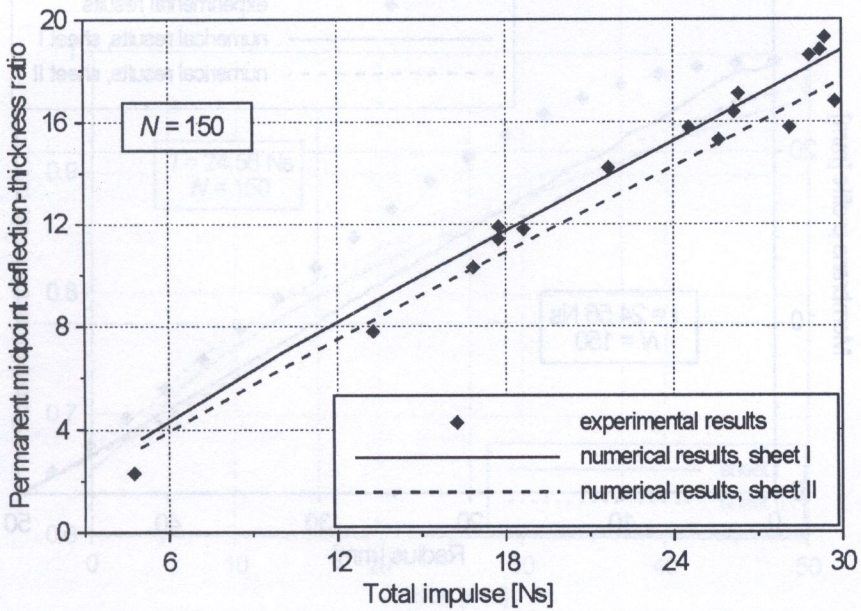


FIG. 7. Permanent midpoint deflection-thickness ratio versus total impulse.

The predicted membrane deflection shapes for $I = 24.56\text{Ns}$ are shown in Fig. 8, where comparison is made for two different sets of material parameters. For both cases, it can be seen that the predicted shape does not correspond very well to the experimental shape. It appears that this visible disagreement between the theoretical shapes and the shape measured experimentally, results directly from the membrane formulation in which the bending forces are neglected. The analysis of a deformation process for plates loaded impulsively presented in [7] shows that the initial phase of motion is dominated by the strong bending effects. At last these effects have to influence the final shape of the plate. However, such a deformed shape reminding the cone motivates the approximate membrane solution in which the linear shape function is used, see Duffey [10].

The dynamic, elasto-viscoplastic response of the membrane can be characterized also by the history of the membrane force. Such a history for the membrane force-yield force ratio at the midpoint is shown in Fig. 9. The value of the first amplitude of the membrane force exceeding the corresponding value $N_0 = \sigma_0 H$ gives evidence on the hardening degree due to the viscoplastic effects. After a long period (more or less $100\ \mu\text{s}$) of the fixed viscoplastic flow we can observe a fast unloading of the central cross-section, and next the irregular, elasto-viscoplastic vibrations with the decreasing amplitude.

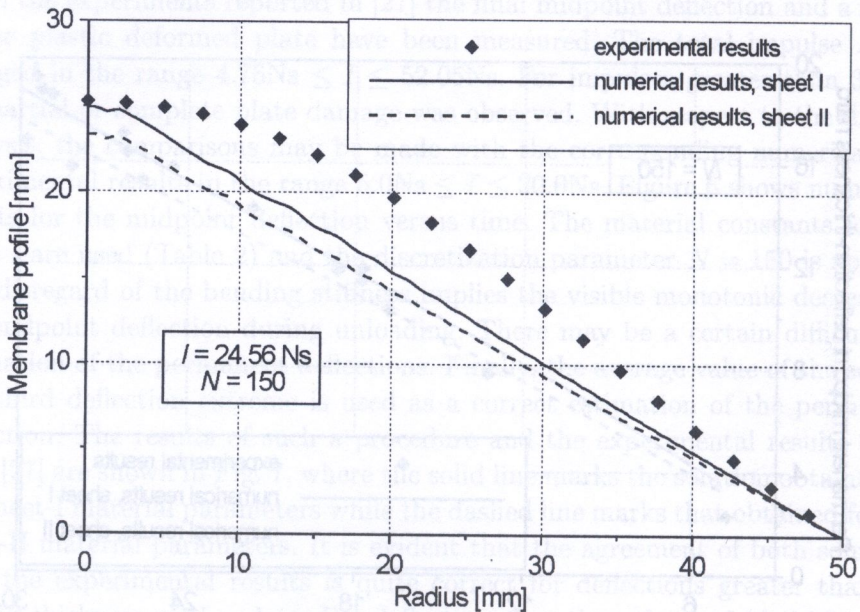


FIG. 8. Comparison between experimental and predicted membrane deflection shapes.

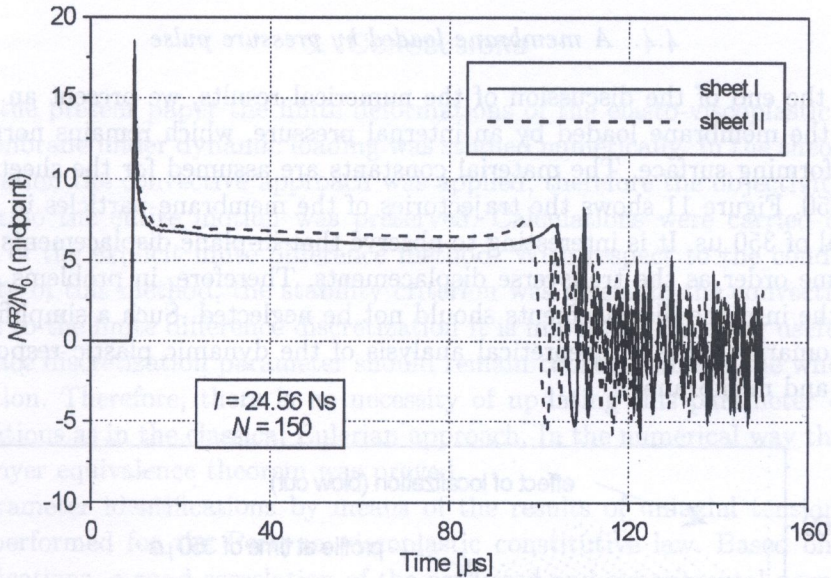


FIG. 9. Variation in time of the membrane force-yield force ratio at the midpoint.

The permanent distribution of the actual-initial thickness ratio along the radial cross-section of the same membrane is shown in Fig. 10. There is the largest decrease (about 35 % of the initial value) of the thickness in the area around the membrane center.

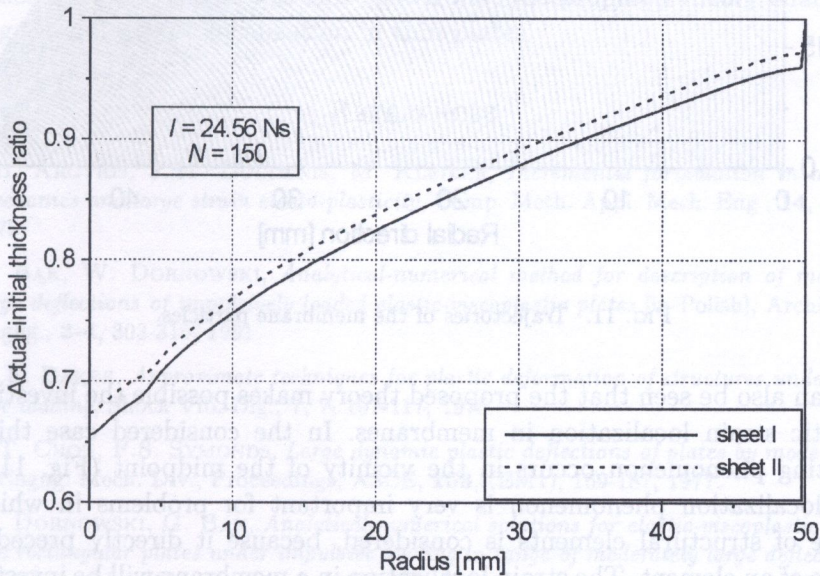


FIG. 10. Distribution of the actual-initial thickness ratio along the radial cross-section.

4.4. A membrane loaded by pressure pulse

At the end of the discussion of the numerical results, we present an example of the membrane loaded by an internal pressure, which remains normal to the deforming surface. The material constants are assumed for the sheet I and $N = 250$. Figure 11 shows the trajectories of the membrane particles in a time interval of $350 \mu\text{s}$. It is interesting to observe that in-plane displacements are of the same order as the transverse displacements. Therefore, in problems of this type, the in-plane displacements should not be neglected. Such a simplification is customarily made in theoretical analysis of the dynamic plastic response of plates and membranes.

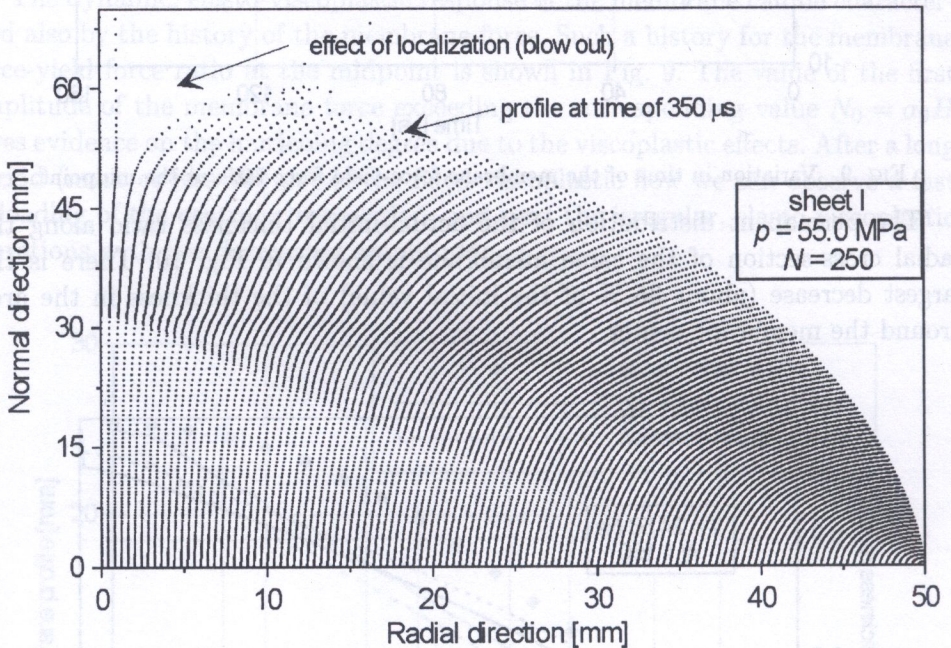


FIG. 11. Trajectories of the membrane particles.

It can also be seen that the proposed theory makes possible the investigation of plastic strain localization in membranes. In the considered case this very interesting phenomenon occurs in the vicinity of the midpoint (Fig. 11). The strain localization phenomenon is very important for problems in which the fracture of structural elements is considered, because it directly precedes the fracture of an element. The strain localization in a membrane will be investigated more exactly in other publication. The results presented here should be treated as introductory.

5. CONCLUSIONS

In the present paper the finite deformations of the elasto-viscoplastic circular membrane under dynamic loading was studied numerically. In the theoretical formulation the convective approach was applied, therefore the objectivity with respect to the entire motion was preserved. Calculations were carried out by means of the explicit finite difference method. With respect to the conditional stability of this method, the stability criterion was given. In the convective approach to the finite difference discretization it is important and very useful that the space discretization parameter should remain constant during the whole deformation. Therefore, there is no necessity of updating this parameter during calculations as in the classical Eulerian approach. In the numerical way the Lax-Richtmyer equivalence theorem was proved.

Parameter identifications by means of the results of uniaxial tension tests were performed for the Perzyna viscoplastic constitutive law. Based on these identifications, a good correlation of the predicted and experimental permanent deflections was achieved over the range of the midpoint deflection-thickness ratio up to 20. The impulse transverse velocity distributed uniformly over the entire surface was considered. It was found that certain disagreement between the membrane shape determined numerically and that measured experimentally results directly from the membrane formulation in which the bending effects are neglected. In the considerations, the thickness change during the deformation was taken into account. It was also shown that the proposed theory enables the investigation of plastic localization in thin plates.

REFERENCES

1. J.H. ARGYRIS, J.ST. DOLTSINIS, M. KLEIBER, *Incremental formulation in nonlinear mechanics and large strain elasto-plasticity*, Comp. Meth. Appl. Mech. Eng., **14**, 259-294, 1978.
2. G. BAŁ, W. DORNOWSKI, *Analytical-numerical method for description of moderately large deflections of impulsively loaded elastic-viscoplastic plates* [in Polish], Archives Civ. Engng., **3-4**, 303-315, 1991.
3. W.E. BAKER, *Approximate techniques for plastic deformation of structures under impulsive loading*, Shock Vib. Dig., **7**, 7, 107-117, 1975.
4. C.T. CHON, P.S. SYMONDS, *Large dynamic plastic deflections of plates by mode method*, J. Engng. Mech. Div., Proceedings, ASCE, **103**, (EM1), 169-187, 1977.
5. W. DORNOWSKI, G. BAŁ, *Analytical-numerical solutions for elastic-viscoplastic circular and rectangular plates under impulsive loading in range of moderately large deflections* [in Polish], Archives Civ. Engng., **3-4**, 373-392, 1991.
6. W. DORNOWSKI, *Finite deformations of elasto-plastic membranes loaded dynamically* [in Polish], Bull. MUT, **2**, 498, 85-97, 1994.

7. W. DORNOWSKI, *Interaction of membrane and bending forces in plates at nonlinear vibrations*, Engng. Trans., **42**, 1-2, 33-59, 1994.
8. W. DORNOWSKI, *Numerical simulation of plastic flow processes under dynamic cyclic loadings* [in Polish], MUT report, 2598/99, Warszawa 1999.
9. W. DORNOWSKI, P. PERZYNA, *Localization phenomena in thermo-viscoplastic flow processes under cyclic dynamic loadings*, Computer Assisted Mechanics and Engineering Sciences, **7**, 117-160, 2000.
10. T.A. DUFFEY, *The large deflection dynamic response of clamped circular plates subject to explosive loading*, Sandia Laboratories Research Report No. SC-RR-67-532, 1967.
11. A.E. GREEN, W. ZERNA, *Theoretical elasticity*, Second Edition, Clarendon Press, Oxford 1960.
12. C. GUEDES SOARES, *A mode solution for the finite deflections of a circular plate loaded impulsively*, Engng. Trans., **29**, 99-114, 1981.
13. R. HILL, *Aspects of invariance in solid mechanics*, Advances in Applied Mechanics, **18**, 1-75, 1978.
14. M. KLEIBER, C. WOŹNIAK, *Nonlinear mechanics of structures*, PWN Warszawa, Kluwer Academic Publishers Dordrecht/Boston/London, 1991.
15. P. KŁOSOWSKI, K. WOŹNICA, D. WEICHERT, *Dynamics of elasto-viscoplastic plates and shells*, Archive Appl. Mech., **65**, 326-345, 1995.
16. J.W. LEECH, E.A. WITMER, T.H.H. PIAN, *Numerical calculation technique for large elastic-plastic transient deformations of thin shells*, AIAA J., **12**, 6, 2352-2359, 1968.
17. H. LIPPMANN, *Kinetics of the axisymmetric rigid-plastic membrane supplied to initial impact*, Int. J. Mech. Sci., **16**, 297-303, 945-947, 1974.
18. J.E. MARSDEN, T.J.R. HUGHES, *Mathematical foundations of elasticity*, Prentice-Hall, Englewood Cliffs, NJ, 1983.
19. J.B. MARTIN, P.S. SYMONDS, *Mode approximations for impulsively loaded rigid-plastic structures*, J. Engng. Mech. Div., Proceedings, ASCE, **92**, (EM5), 43-66, 1966.
20. A. NEEDLEMAN, V. TVERGAARD, *Finite element analysis of localization plasticity*, [in:] Finite Elements, Vol. V: Special problems in solid mechanics, J.T. ODEN and G.F. CAREY [Eds.], Prentice-Hall, Englewood Cliffs, New Jersey 1984.
21. G.N. NURICK, H.T. PEARCE, J.B. MARTIN, *The deformation of thin plates subjected to impulsive loading*, [in:] Inelastic Behaviour of Plates and Shells, L. BEVILACQUA [Ed.], Springer Verlag, New York 1986.
22. N. PERRONE, P. BHADRA, *Simplified large deflection mode solutions for impulsively loaded viscoplastic circular membranes*, J. Appl. Mech., **51**, 505-509, 1984.
23. P. PERZYNA, *Internal state variable description of dynamic fracture of ductile solids*, Int. J. Solids Struct., **22**, 7, 797-818, 1986.
24. R.D. RICHTMYER, K.W. MORTON, *Difference methods for initial-value problems*, John Wiley, New York, 1967.
25. M. STOFFEL, R. SCHMIDT, D. WEICHERT, *Shock wave-loaded plates*, Int. J. Solids Struct., 2001 (in press).

26. P.S. SYMONDS, T. WIERZBICKI, *Membrane mode solution for impulsively loaded circular plates*, J. Appl. Mech., **46**, 58-64, 1979.
27. R.G. TEELING-SMITH, G.N. NURICK, *The deformations and tearing of thin circular plates subjected to impulsive loads*, Int. J. Impact Engng, **11**, 1, 77-91, 1991.
28. E.A. WITMER, H.A. BALMER, J.W. LEECH, T.H.H. PIAN, *Large dynamic deformations of beams, circular rings, circular plates and shells*, AIAA J., **1**, 8, 1848-1857, 1963.
29. C. WOŹNIAK, *Nonlinear theory of shells* [in Polish], PWN, Warszawa 1966.

Received November 16, 2001.

U. Audreani, P. Casini and P. Vestrini

Dipartimento di Ingegneria Strutturale e Geotecnica,
Università degli Studi di Roma "La Sapienza",
10 Via Eudossiana, 00184 Roma
e-mail: geal.casini@uniroma1.it

The presence of a crack could not only cause a local variation in the stiffness, but it could affect the mechanical behaviour of the entire structure to a considerable extent. The frequencies of natural vibrations, amplitudes of forced vibrations and stress of dynamic starting change due to the existence of such cracks. The vibration characteristics of cracked structures can be useful for non-destructive testing. In particular, the natural frequencies and mode shapes of cracked beams can provide insight into the extent of damage. The beam has been schematized as a 2-D continuous medium and discretized by means of quadrilateral finite elements. The lowest three natural frequencies (and the associated mode shapes) of the cracked cantilever beam were obtained via both the modal and spectral analyses, and were compared with experimental data from literature in order to assess the reliability of different models of crack state, namely open crack and contact crack. Both the experimental and analytical results reveal the significant influence of the opening and closing conditions of the crack on the frequency reduction; namely this reduction decreases as more realistic contact phenomena are considered at crack interfaces.

1. INTRODUCTION

Although machines and structures are carefully designed for fatigue loading, possess high levels of safety, are constructed with high quality materials, and thoroughly inspected prior to service as well as periodically during their operating lives, still there are instances of cracks or damage escaping inspections. Therefore, the development of structural integrity monitoring techniques have received increasing attention in recent years [6]. Among these monitoring techniques, it is believed that the monitoring of the global dynamics of a structure offers favourable alternative if the on-line (in service) damage detection is